

Fabrication and characterization of efficient hybrid photocatalysts based on titania and graphene for acid orange seven dye degradation under UV irradiation

P. Muthirulan, C. K. N. Devi, M. M. Sundaram*

Centre for Research and Post-Graduate Studies in Chemistry, Ayya Nadar Janaki Ammal College (Autonomous), Sivakasi 626 124, TN, India

*Corresponding author: Tel.: (+91) 9486028616; Fax: (+91) 4562254970; E-mail: drmmmsundaram61@gmail.com; chemistryanjac@gmail.com

Received: 13 July 2013, Revised: 22 August 2013 and Accepted: 01 September 2013

ABSTRACT

Simple and proficient methodology has been proposed for the preparation of hybrid photocatalyst based on titanium dioxide (TiO₂)-graphene (GR) nanocomposite for acid orange 7 (AO7) dye degradation under UV irradiation. High Resolution Transmission Electron Microscopy (HRTEM) and Scanning Electron Microscopy (SEM) studies revealed that TiO₂ nanoparticles were uniformly dispersed on GR surface. TiO₂-GR hybrid nanocomposite has also been characterized by Ultraviolet Diffusive Reflectance Spectroscopy (UV-DRS), Raman spectroscopy and X-ray diffraction (XRD) studies. Electrochemical Impedance spectroscopy (EIS) measurement revealed that the incorporation of GR with TiO₂ nanoparticles significantly enhanced the electrical conductivity. The peak intensity of PL spectra of GR containing catalysts are lower than that of pristine TiO₂, indicating that the electron-hole recombination rate of self-trapped excitations in TiO₂ is reduced by the introduction of GR. The photocatalytic degradation measurements demonstrated that the TiO₂-GR composites exhibited an enhanced photocatalytic activity for AO7 degradation under UV irradiation compared to pure TiO₂. This may be due to greater adsorptivity of dyes, extended light absorption and increased charge separation efficiency due to excellent electrical properties of graphene and the large surface contact between graphene and TiO₂ nanoparticles. Therefore, the TiO₂-GR composites can be widely used as a ternary composite photocatalyst for treating the organic contaminant in the field of environmental protection. Copyright © 2014 VBRI press.

Keywords: TiO₂-GR nanocomposites; hybrid photocatalyst; acid orange 7; UV irradiation; photocatalysis.



P. Muthirulan is currently working as a Project Fellow in the UGC-MRP Project at Centre for Research and PG Studies in Chemistry, Ayya Nadar Janaki Ammal College, Sivakasi, TN, India. He received his Bachelor of Science, Master of Science and Master of Philosophy Degrees in Chemistry from Madurai Kamaraj University, Madurai. P. Muthirulan received various prestigious fellowships and awards including Young Researcher, Research Fellow/Associate from UGC, DST (SRF) and CSIR (SRF), India. He has submitted his Ph. D thesis for review. His research area is mainly on Development of functional nanomaterials and nanocomposites for multifunction applications. He has published more than 20 research articles in the reputed International/National Journals and Conference Proceedings.



C. Nirmala Devi is currently doing M. Phil., degree course at Centre for Research and PG Studies in Chemistry, Ayya Nadar Janaki Ammal College, Sivakasi, TN, India. She

received her Bachelor of Science and Master of Science Degrees in Chemistry from Madurai Kamaraj University, Madurai. She has submitted her M. Phil., dissertation for review. Moreover, She has published two research articles internationally reputed Journal. Besides, she has presented her findings in many International/National conferences/seminar/symposia.



M. Meenakshi Sundaram is an Associate Professor and Head of Centre for Research and PG Studies in Chemistry, Ayya Nadar Janaki Ammal College, Sivakasi, TN, India. His main research activities include the synthesis and fabrication of advanced materials/composites at nanoscale for waste water treatments and corrosion protection. His current research is focused on synthesis of conducting polymer based nanocomposites for photocatalysis, solar and fuel cells. He has published more than 30 research articles in journals of International/National repute. He has completed TNSCST, UGC, DST funded Research Projects and one is ongoing to his credit.

Introduction

Heterogeneous photocatalytic oxidation has been studied for several decades and shown to be an effective method for dealing with the environmental pollution problems, such as air cleanup, water disinfection, hazardous waste remediation, and water purification. Among various semiconductor photocatalysts, titania has attracted much attention due to its fascinating properties such as biological and chemical inertness, strong oxidizing power, cost-effective, and long-term stability against photocorrosion and chemical corrosions. However, the high rate of electron-hole recombination in TiO₂ particles results in low quantum efficiency of photocatalytic reactions. Therefore, increasing the photocatalytic activity of TiO₂ is of great interest for the practical applications. To date, a variety of strategies have been utilized to improve the photocatalytic performance of TiO₂ [1-5].

In the recent years, significant interest has been devoted to designing semiconductor-Graphene composite materials, aiming at a synergetic combination of their intrinsic outstanding properties and, thus, enhanced performance to meet new requirements imposed by specific applications, such as solar energy utilization, optoelectronic quantum dot arrays, and heterogeneous photocatalysis [6-8]. Indeed, some studies have proven that the electron accepting and transport properties of GR provide a convenient way to direct the flow of photogenerated charge carriers, which thus increases the lifetime of electron-hole pairs generated by semiconductors upon light irradiation. Consequently, the photocatalytic activity of semiconductors will be improved for target reactions. Most recently, synthesis and fabrication of TiO₂-GR nanocomposites by different methodologies has been reported by various authors for the applications of photodegradation of dyes and other organic pollutants [9-12].

However, it should be noted that most of them were based on nonaqueous synthesis and lengthy experimental procedure, which limited their practical application. Furthermore, all precursors used in aforementioned works were unstable in water phase or sensitive to air which limited the TiO₂ loading amount and photocatalytic abilities of as-prepared composites.

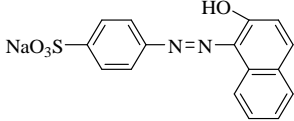
Therefore, novel and environmental-friendly approaches to preparation of homogenous colloidal suspensions of high-quality TiO₂-GR composite remain a great challenge. In the present study describes the fabrication of TiO₂-GR nanocomposite by simple approach for the application of AO7 dye degradation under UV irradiation. The prepared TiO₂-GR nanocomposite was characterized by HRTEM, FESEM, UV-DRS, Raman spectroscopy, XRD, PL and EIS studies. Plausible explanation and mechanism for the photodegradation has also been predicted.

Experimental

Chemicals and reagents

Titanium dioxide nanoparticle was purchased from Sigma-Aldrich with the particles size of ~20nm. AnalaR grade of acid orange 7 (AO7) dye was purchased from E. Merck,

India and it was used as a model pollutant. The physicochemical properties of AO7 dye was as follows-

Dye	Acid Orange 7
CI No.	15510
Characteristics	Anionic, water soluble
Formula	C ₁₆ H ₁₁ N ₂ NaO ₄ S; MW : 350.32
Structure	
λ_{\max}	483 nm
Applications	Nylon, wool, polyester, cellulose

All the other chemicals and reagents were of AnalaR grade supplied by BDH, India, Ranbaxy and SD fine chemicals. All the reagents and solutions were prepared using Double Distilled (DD) water.

Preparation of TiO₂-GR nanocomposites

The TiO₂-GR composites were prepared by based on our earlier reports [13, 14]. The procedure is as follows: 100mL suspension of ethanol in 70 mg of TiO₂ nanoparticles were mixed with 30 mg of GR followed by ultrasonication for 30 min. in order to get uniform dispersion and then the suspension is transferred in a rotary evaporator under vacuum for 45 min. After the rotation, the ethanol is evaporated out and dried. Before each photocatalysis experimental studies, the TiO₂-GR nanocomposite is activated and dried at 100°C for 1 hr and this composite is used as a photocatalyst.

Instrumentations

HRTEM was carried out on a TECNAI-G (model T- 30) S-twin high resolution transmission electron microscope operated at an accelerating voltage of 300 kV. The surface morphology of the TiO₂-GR was observed with a FESEM HITACHI SU6600 instrument with an accelerating voltage of 1.5 kV.

UV-*vis* adsorption and reflectance spectra were recorded using "TECHCOMP" UV-visible spectrometer model 8500. Raman experiments were performed on Raman 11i (Nanophoton Corporation, Japan) using 532 nm excitation line from a He-Ne laser with a laser power about 1.2 mW on the sample surface. The X-ray powder diffraction patterns of the samples were recorded at room temperature by Bruker D8 Advance X-ray diffraction system with Cu-K α radiation.

The electrochemical experiments were carried out with the PGSTAT-12 electrochemical Analyzer (AUTOLAB, The Netherlands BV) using glassy carbon (GC) as working electrode a Pt wire in the form of a spiral with high geometrical surface area (~ 20 cm²) was used as a counter electrode and standard calomel electrode (SCE) as reference electrode. The nanocomposites electrode preparation is as follows: 2.0mg TiO₂-GR nanocomposite as

dispersed in 5 mL of 0.5% nafion in ethanolic solution by ultrasonic agitation for 10 minutes in order to get homogeneous suspension. 5 μ l of the TiO₂-GRnanocomposite suspension was drop casted on to the GCE and it was allowed to dry for 30 min at room temperature. Identical experimental procedure was adopted for making TiO₂-GC modified electrode.

The photodegradation experiments were carried out in a 50 ml cylindrical glass reactor (HEBER Multilamp Photoreactor) equipped with an UV lamp (365 nm). The concentration of residual AO7 was determined by visible spectrophotometer (ELICO SL 207 MINI SPEC) based on the absorbance at the wavelength of 483 nm. The pH of the dye solution was measured by using digital pen pH meter (Hanna instrument, Portugal).

Photodegradation experiments

The photocatalytic activities of the photocatalysts were evaluated by photodegradation of AO7 in an aqueous solution under UV- light. Stock solution of dye (3000 ppm of AO7) was suitably diluted to the required initial concentration of dye with DD water. 50 mL of the dye solution of known concentration was taken in photoreactor vessel. Required amount of catalyst (TiO₂ or TiO₂-GR nanocomposite) was exactly weighed and then transferred into the photoreactor vessel. The photoreactor vessel was then placed in the safety hood. Before illumination was turned on the suspension was stirred with magnetic stirrer in order to obtain adsorption-desorption equilibrium processes. Samples of the suspension was withdrawn regularly from the reactor at different time intervals and centrifuged for separation of the suspended solids. The clean transparent solution was analyzed by spectrophotometric technique by measuring the absorbance using visible spectrophotometer [13, 14].

In the photodegradation experiments the extent of removal of the dye, in terms of the values of percentage removal has been calculated using the following relationship:

$$\text{Percentage removal (\%R)} = 100 \cdot (C_i - C_f) / C_i \quad (1)$$

where, C_i = initial concentration of dye (ppm); C_f = final concentration of dye (ppm) at given time.

Results and discussion

Surface morphology of TiO₂-GR nanocomposite

Surface morphological and structural features of the TiO₂-GR nanocomposite were examined by HRTEM as depicted in Fig. 1. The wrinkles on the GR sheets are clearly observed (Fig. 1 (A)). It is clear that from Fig. 1 (B) that the TiO₂ nanoparticles are uniformly dispersed on the GR surface. Moreover, TiO₂ can sufficiently interact with the functional groups of well-dispersed GR in an aqueous phase, thereby leading to the intimate integration of the GR sheet and TiO₂ ingredients. In this case, the excellent electron conductivity of GR is able to be utilized efficiently, thus enhancing the lifetime of photogenerated electron hole pairs more effectively. This in turn leads to

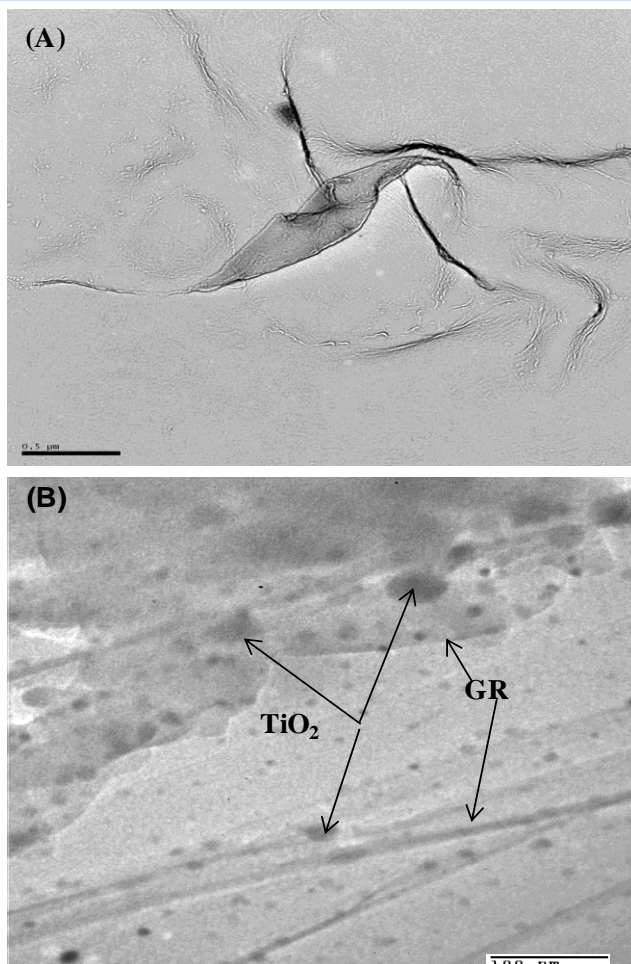


Fig. 1. HRTEM images of (A) GR and (B) TiO₂-GR nanocomposite.

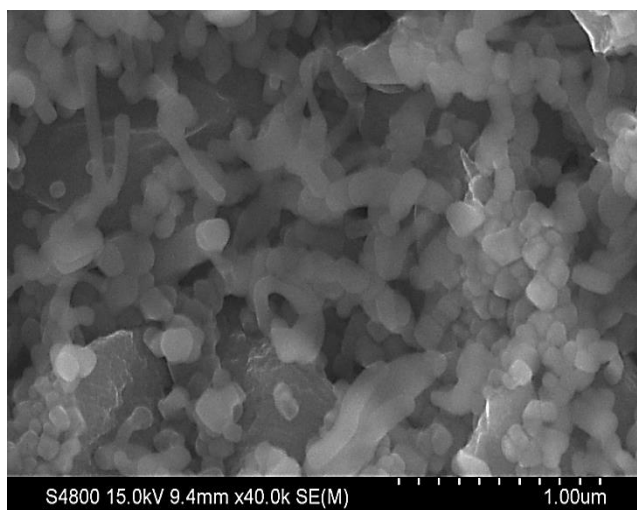


Fig. 2. FESEM image TiO₂-GR nanocomposite.

the observation of much higher photocatalytic activity of TiO₂-GR towards photocatalytic degradation of AO7 dye. Fig. 2 shows the SEM image of TiO₂-GR nanocomposite. It is clear from SEM picture that the two dimensional structure of GR sheets with micrometers long wrinkles is still retained in TiO₂-GR nanocomposites and the GR sheets are well decorated by the spherical shaped TiO₂ nanoparticles [15, 16].

UV-DRS measurements

The band electronic structure of a photocatalytic material usually has a dominant effect in its photocatalytic activity. In this study, the influence of the introduction of graphene on the band gap energy of TiO_2 was studied by the optical response of the as-prepared TiO_2 -GR nanocomposites through UV-DRS. **Fig. 3** shows the UV-DRS of the as-prepared TiO_2 -GR nanocomposites and TiO_2 samples. Compared with pure TiO_2 , the absorption band of TiO_2 -GR nanocomposites had a slight redshift and this result is caused by the hybridization of C2p and O2p atomic orbits to form a new valence band. Thus, the band gap energy was reduced in the TiO_2 -GR nanocomposites system [17, 18].

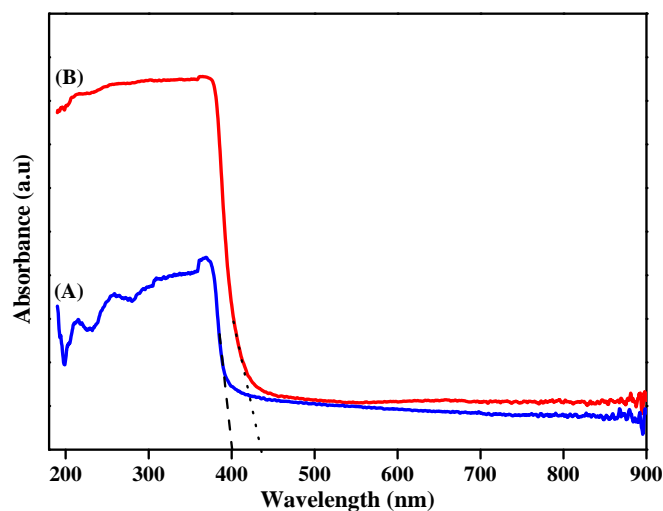


Fig. 3. UV-DRS spectra of (A) TiO_2 and (B) TiO_2 -GR nanocomposite.

Raman spectral studies

Fig. 4 shows the Raman spectra of GR, pure TiO_2 and TiO_2 -GR nanocomposite. In the case of GR, there are two typical Raman bands located at -1100 and 1596 cm^{-1} , which correspond to disordered sp^2 carbon (D-band) and well-ordered graphite (G-band), respectively. As for pure TiO_2 , several characteristic bands at 146 , 397 , 516 , and 637 cm^{-1} corresponds to the $\text{Eg}(1)$, $\text{B1g}(1)$, $\text{A1g} + \text{B1g}(2)$ and $\text{Eg}(2)$ modes of anatase, respectively. For the TiO_2 -GR nanocomposites, all the Raman bands for anatase can be observed suggesting that the structure of graphene is maintained in the composite [15-18].

X-ray diffraction pattern

The crystallographic structure of the as obtained TiO_2 -GR nanocomposite was evinced by XRD measurements. **Fig. 5** shows the XRD pattern of the mere TiO_2 and TiO_2 -GR nanocomposites. The XRD pattern of the GR shows broad diffraction peak at 25.9° which can be indexed to (002) diffraction for typical graphite carbon. The peaks located at 25.3 , 37.8 , 48.0 , 53.9 , and 55.1° can be indexed to (101), (004), (200), (105), and (211) crystal planes of anatase TiO_2 [JCPDS no. 21-1272]. However, the diffraction peaks of GR are not distinguishable in XRD patterns of TiO_2 -graphene. This phenomenon has also been observed in

other relevant works, and it can be ascribed to the much lower crystalline extent of graphene than that of TiO_2 , which results in the shielding of the GR peaks by those of TiO_2 . These features indicate that the modification with GR did not influence the lattice structure of TiO_2 [19-23].

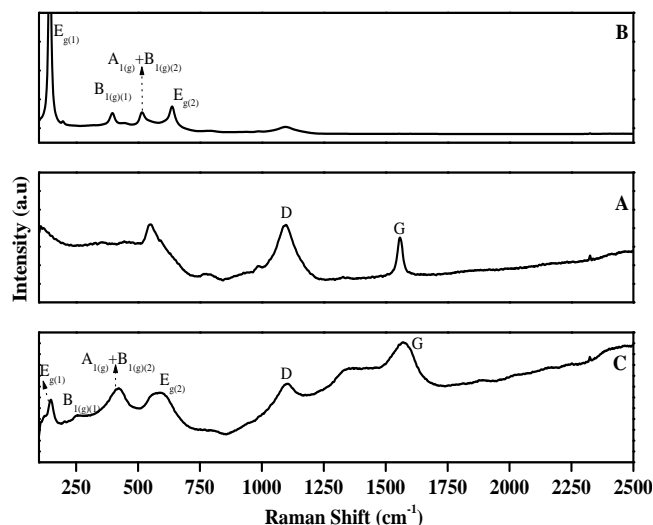


Fig. 4. Raman spectra of (A) GR, (B) TiO_2 and (C) TiO_2 -GR nanocomposite.

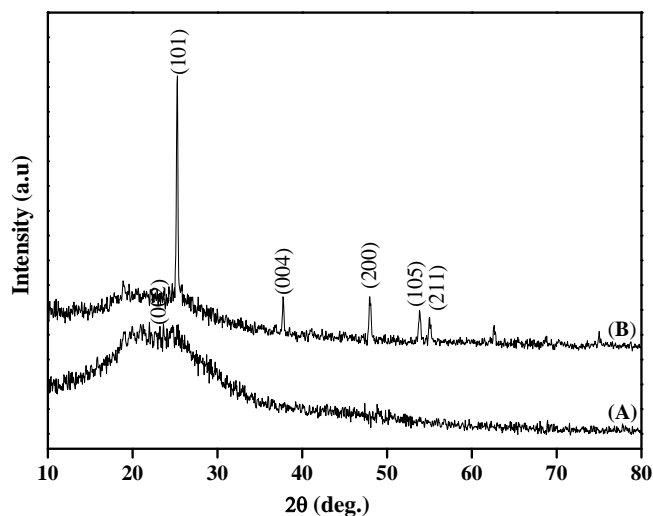


Fig. 5. XRD pattern of (A) GR and (B) TiO_2 -GR nanocomposite.

Electrochemical impedance spectroscopy measurements

Electrochemical impedance spectroscopy is an extremely powerful and sensitive characterization technique for probing the electron-transfer kinetics occurring at surface-modified electrodes. The EIS spectra of bare GC, TiO_2 -GC and GR- TiO_2 /GR nanocomposites modified electrodes are shown in **Fig. 6**. The bare GCE represents a semicircle at high frequencies, followed by a near vertical line at low frequencies. The semicircle at high frequencies is related to the faradaic process (interfacial charge transfer resistance) occurred at the electrode/electrolyte interface indicated the low electron transfer rate. When, TiO_2 was assembled on the GC electrode, the semicircle increased dramatically, suggesting that TiO_2 blocked the electron exchange

between the redox probe and electrode surface. However, upon the incorporation of GR on the TiO₂/GCE, the semicircle or electron-transfer resistance almost disappeared obviously and suggesting that the presence of GR made the electron transfer easier. This may be attributed to the good promotion of interfacial electron transfer between the electrode and the electrolyte interface by GR. These results confirmed that the incorporation of GR with TiO₂ makes it easier for the fascination of electron transfer process and electrical conductivity [24, 25].

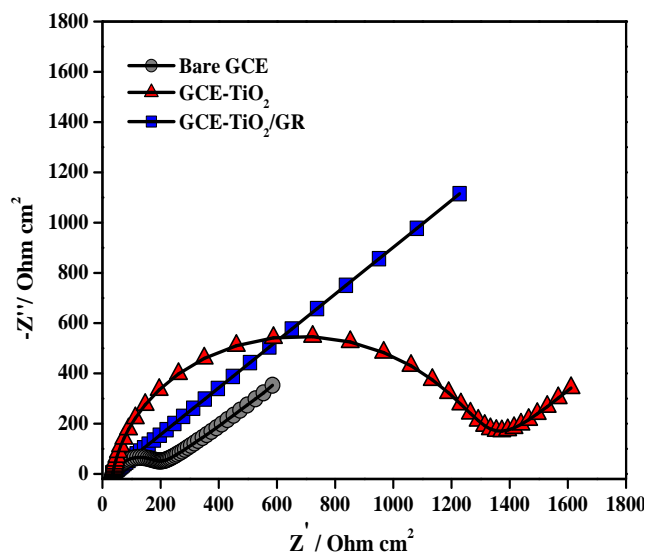


Fig. 6. Nyquist plots of bare GC, TiO₂/GC and TiO₂-GR nanocomposite/GC modified electrode in 0.1 M KCl containing 2 mM of K₃[Fe(CN)₆] solution.

The important role of graphene in the TiO₂-GR nanocomposites is the electron acceptor and transporter. On the one hand, GR has been reported to be a competitive candidate for the acceptor material due to its two dimensional π -conjugation structure, and in the TiO₂-GR nanocomposites, the excited electrons of TiO₂ could transfer from the conduction band to graphene *via* a percolation mechanism. Thus, in TiO₂-GR nanocomposites, GR served as an acceptor of the generated electrons of TiO₂ and effectively suppressed the charge recombination, leaving more charge carriers to form reactive species and promote the degradation of dyes. On the other hand, GR has unexpectedly excellent conductivity due to its two-dimensional planar structure. Therefore, the rapid transport of charge carriers could be achieved and an effective charge separation subsequently accomplished.

PL studies

The photoluminescence emission spectrum has been widely used to investigate the efficiency of charge carrier trapping, immigration and transfer, and to understand the fate of e⁻/h⁺ pairs in semiconductor particles. With the recombination of e⁻/h⁺ after a photocatalyst is irradiated, photons are emitted, resulting in the photoluminescence. This behavior is attributed to the reverse radiative deactivation from the excited-state of Ti species. The PL spectra of the TiO₂ and TiO₂-GR nanocomposite were

presented in **Fig. 7**. As anticipated, the pristine TiO₂ photocatalyst shows a broad PL emission band, which is similar to that reported in the literature. The peak intensities of PL spectra of TiO₂-GR nanocomposite was lower than that of TiO₂, indicating that the electron-hole recombination rate of self-trapped excitation in TiO₂ is reduced by the introduction of GR. The significant PL quenching of TiO₂ can be observed after combination with GR, indicating the effective transfer of photo-generated electron from the TiO₂ to GR, leading to the improved photocatalytic activity of the TiO₂-GR nanocomposites [22, 23].

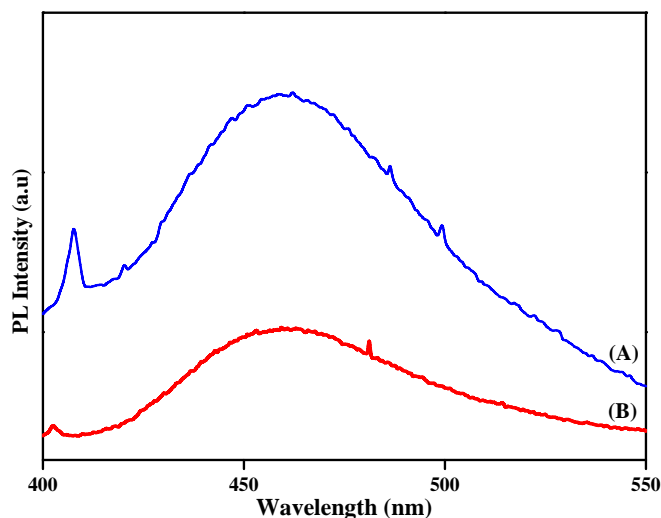


Fig. 7. PL spectra of (A) TiO₂ and (B) TiO₂-GR nanocomposite.

Photodegradation studies

Effect of initial concentration on the photodegradation of AO7 dye under UV irradiation: The effect of concentration on the percentage degradation was studied by varying the initial concentration of AO7 dye from 10ppm to 60ppm with optimum catalyst loading (10mg) and irradiation time (60min.). The results are shown in **Fig. 8**. The results indicate that the TiO₂-GR nanocomposites photocatalyst showed greater degradation ability towards AO7 than TiO₂. It was also found that the percentage degradation decreases with increasing initial concentration of the dye for both the catalysts. It has been indicated in several investigations that as the concentration of the target pollutant increases, more and more molecules of the compound are adsorbed on the surface of the photocatalyst. Therefore, the reactive species ([•]OH and [•]O₂) required for the degradation of the pollutant also increases. However, the formation of [•]OH and [•]O₂ on the catalyst surface remains constant for a given light intensity, catalyst amount and duration of irradiation. Hence, the available OH radicals are inadequate for AO7 dye degradation at higher concentrations. Consequently the AO7 dye percentage of removal decreases as the concentration increases. In addition, an increase in substrate concentration can lead to the generation of intermediates, which may adsorb on the surface of the catalyst. Slow diffusion of the generated intermediates from the catalyst surface can result in the deactivation of active sites on the photocatalyst and result

in a reduction in the degradation rate. In contrast, at low concentrations, the number of catalytic sites will not be the limiting factor and the rate of degradation will be proportional to the substrate concentration [13, 14, 26-28]. The optimum concentration of dye was found to be 30 ppm.

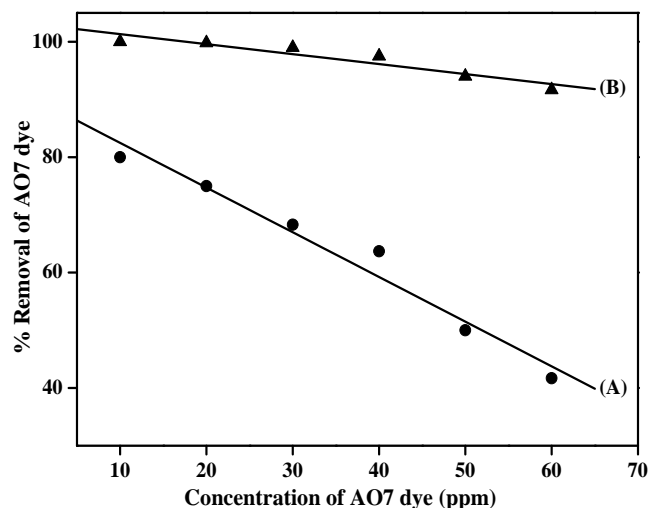


Fig. 8. Effect of initial concentration on the photodegradation of AO7 dye under UV irradiation in the presence of TiO₂ and TiO₂-GR nanocomposite [Irradiation Time: 45min.; Dose: 10mg; pH: 3.7].

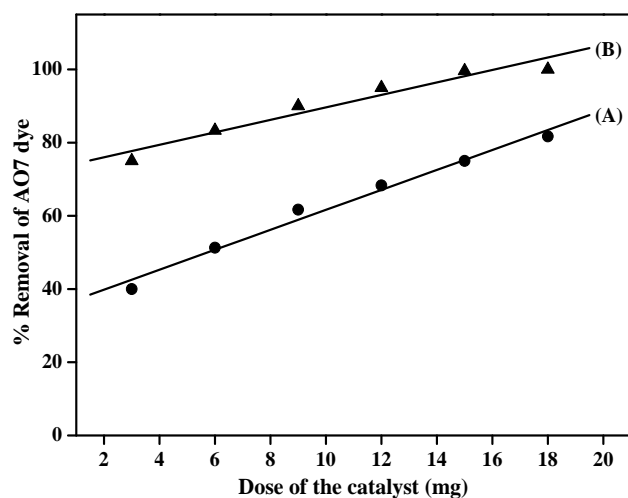


Fig. 9. Effect of dose of the photocatalyst on the photodegradation of AO7 dye under UV irradiation in the presence of mere TiO₂ and TiO₂-GR nanocomposite [AO7 concentration: 30ppm; Irradiation Time: 45min.; pH: 3.7].

Influence of photocatalyst dose on the photodegradation of AO7 dye: The optimization of the catalyst dosage is necessary in order to avoid excess catalyst and also to ensure total absorption of photons for efficient photomineralization. Experiments were performed by varying the amount of catalysts from 3-18mg/50mL. The obtained results were **Fig. 9**. The percentage of removal increases with increase in dose of the catalysts from 45 to 81.7% for TiO₂/UV system and from 75 to 99.99% for TiO₂-GR/UV system. Irrespective of the nature of the dye and photocatalysts, the percentage of removal

was found to enhance linearly with increase in the dose of the catalyst indicating the heterogeneous regime.

This may probably be due to: (i) increase in the extent of dye adsorption molecules on the catalyst surface; (ii) increase in the number of surface active sites; (iii) enhanced generation of hydroxyl radicals due to increase in the concentration of charge carriers. However, at higher catalyst loadings (beyond 18mg/50mL), the reaction rate decreased which may be attributed to: (i) the deactivation of activated molecules by collision with ground state molecules; (ii) the agglomeration of the catalyst particles at higher loading which covers the part of photosensitive area retarding the photon absorption and also the dye adsorption; (iii) turbidity at higher catalyst loading results in the shadowing effect thus decreasing the penetration depth of light irradiation; (iv) high degree of scattering by the catalyst particles and increase in the opacity. Hence above a certain level, the additional catalyst amount does not get involved in catalytic activity and further increment in the reaction rate was not observed [13, 14, 18-23]. Hence, the optimum level of dose is 10 mg/50mL.

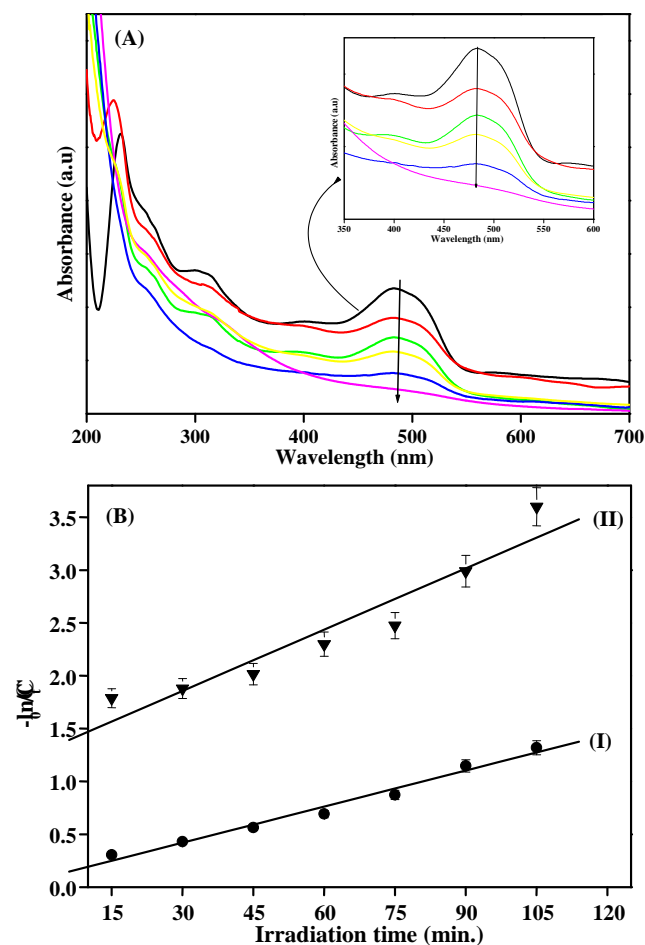


Fig. 10. (A) UV-vis absorption spectra of AO7 dye under UV irradiation with different interval of time [15, 30, 45, 60, 75 and 90 min.] and (B) Photodegradation kinetics of AO dye degradation [AO7 concentration: 30ppm; Dose: 10mg; pH: 3.7].

Assessment of photodegradation kinetics of AO7 dye degradation: Irradiation time plays an important role in the photocatalytic degradation process of AO7 dye. Effect of

irradiation time on the photodegradation of AO7 was carried out with constant dose of the catalyst (10mg/50 mL) and initial concentration (30 ppm) of AO7 dye. It has been observed that the percentage of photodegradation increases with increase in irradiation time and complete degradation was obtained with 90 min. under UV irradiation (Fig. not shown). This may be due to with increase in irradiation time, dye molecules and catalysts have enough time to take part in photocatalytic degradation process and hence percentage of degradation increases.

Fig. 10 (A) depicts the UV-vis absorption spectrum of AO7 dye degradation in the presence of TiO₂-GR nanocomposites by UV irradiation. UV irradiation leads to a continuous decrease in absorbance of AO7 in the presence of TiO₂-GR nanocomposites and the decrease of the absorption band intensities of the dye indicated that dye has been degraded. As can be seen this **Fig. 10 (A)**, the disappearance of the characteristic band of AO7 dye at 483 nm after 90 min. under UV irradiation indicates that AO7 has been degraded completely by TiO₂-GR nanocomposite.

Reaction kinetics gives information about the reaction rates and the mechanisms by which the reactants are converted to the products. It has been agreed that the expression for the rate of decoloration of dye with irradiation under UV light follows the Langmuir-Hinshelwood (L-H) law of heterogeneous photocatalytic reactions. The decoloration kinetics of AO7 in aqueous solution by using UV irradiation was investigated with TiO₂ and TiO₂-GR nanocomposites (**Fig. 10(B)**).

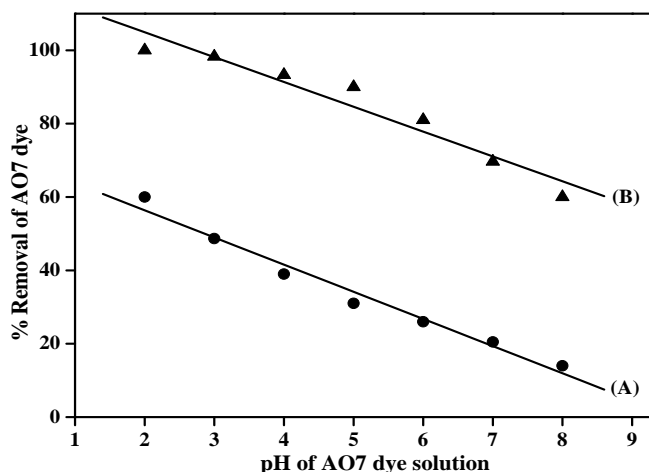


Fig. 11. Effect of pH on the photodegradation of AO7 dye under UV irradiation in the presence of (A) TiO₂ and (B) GR-TiO₂ nanocomposite [AO7 concentration: 30ppm; Irradiation Time: 45min.; Dose: 10mg].

The results of experiments showed that the photocatalytic degradation of AO7 obeys apparently pseudo- first order kinetics and the rate expression is given by the following equation [13, 14, 17-23].

$$\ln C_0/C_t = kt \quad (2)$$

where, C_0 is the initial concentration of AO7; C_t is the concentration of AO7 at time t ; k is the pseudo-first order rate constant and t is the irradiation time respectively. The value of $\ln(C_0/C_t)$ is plotted against time (in min.) and plots are found to be linear. From the slope, the rate constants

were calculated for the degradation of dye AO7 in presence and absence of GR. The pseudo first order rate constant ($k \text{ min}^{-1}$) values of TiO₂ is 0.0263 min^{-1} and TiO₂-GR system is 0.0478 min^{-1} ($R^2 = 0.9392$). The degradation efficiency of the AO7 dye TiO₂-GR nanocomposite is two order magnitudes higher than that of mere TiO₂.

Influence of pH on the photodegradation of AO7 dye

Characteristics of organic pollutants in wastewater differ greatly in several parameters, particularly in their specification behaviour, solubility in water and hydrophobicity. While some compounds are uncharged at common pH conditions typical of natural water or wastewater, other compounds exhibit a wide variation in specification (or charge) and physico-chemical properties. At pH below its pKa value, an organic compound exists as neutral state. Above this pKa value, organic compound attains a negative charge. This variation can also significantly influence their photocatalytic degradation behaviour [13,14].

The point of zero charge (pzc) of TiO₂ is widely reported to be 6.25. Thus, the surface charge density of TiO₂ will be positive below the pzc and negative above it.



The effect of pH on the photocatalytic degradation of AO dye was studied by varying the initial pH of AO7 dye solution from 2 to 7 and keeping constant for all other experimental parameters. It has been observed from **Fig. 11.** that the percentage of photocatalytic decolorization considerably increases with decrease in pH for both light irradiation for TiO₂ and TiO₂-GR nanocomposites. Under acidic pH, the catalyst surface will be positively charged and contains more surface acidic sites. The Lewis base property of AO7 dye renders the molecule to get adsorbed more easily on the catalyst surface. The presence of negatively charged acidic sulfonate group on AO7 dye drives the molecule to adsorb strongly on catalyst surface and hence undergoes faster degradation.

Photodegradation mechanism of AO7 dye

The charge transfer mechanism occurs in TiO₂-GR nanocomposite during photocatalytic degradation of AO7 dye under UV irradiation is shown in **Fig. 12.** When the light irradiated on TiO₂ surface, it generates holes and electrons. In TiO₂, electrons and holes quickly recombine, resulting in low reactivity.

In TiO₂-GR nanocomposite the electrons transfer to GR takes place, since the potential of graphene lies below the conduction band of TiO₂. The graphene sheet promotes the effective charge separation for photo-generated electrons and holes. The trapped electrons on GR can react with the dissolved oxygen to form reactive oxygen species. In this way, electron-hole recombination rate decreases. The photogenerated electrons on the TiO₂ surface could also be trapped directly by the dissolved oxygen to form reactive oxygen species, which react with water to give

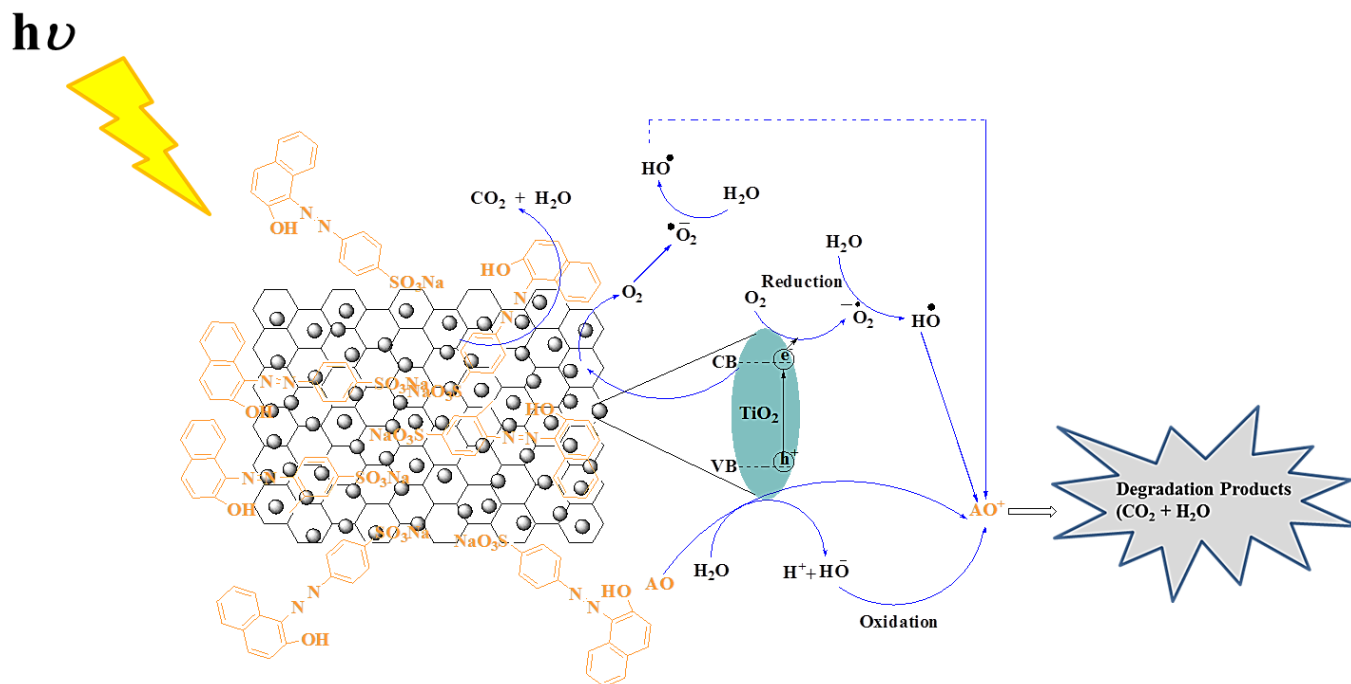
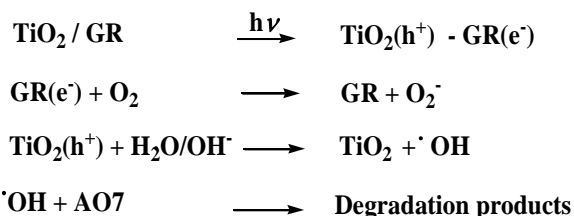


Fig. 12. Schematic illustration on the photodegradation mechanism of the AO7 dye on TiO₂-GR nanocomposite under UV irradiation.

hydroxyl radicals. The dye is then degraded by the hydroxyl groups. On the other hand, holes on the valence band of TiO₂ react with absorbed water or hydroxyl groups to form surface hydroxyl radicals which then degrade dye and the holes can oxidize the dye molecules directly.

The main reactions are shown below:



The photo-generated holes in the VB of TiO₂ used for the photocatalytic degradation of AO7 dye solution. Moreover, holes in TiO₂ react with surface lattice oxygen atoms which are followed by the dissociative adsorption of a water molecule, make the surface becomes super-hydrophilic. TiO₂-GR is efficient to enhance the charge separation of holes and electrons. Due to these holes and electrons transfers, charge recombination suppressed in TiO₂ particles, and hence largely enhances the efficiency of photocatalytic degradation processes [8,9, 15-23].

Conclusion

Effective route and cost-effective strategy for the preparation of TiO₂-GR nanocomposite has been successfully achieved by simple one step chemical process. Microscopy studies revealed that the incorporation of TiO₂ nanoparticles on the GR surface. Spectroscopic studies

evinced that the optimal assembly and interfacial coupling between the reduced GR sheets and TiO₂. The photo-oxidation of AO7 under the UV irradiation followed the pseudo-first-order kinetics according to the Langmuir-Hinshelwood model. Photodegradation studies revealed that TiO₂-GR nanocomposite has higher efficiency in photodegradation of AO7 compared to TiO₂ alone due to the electron transfer between TiO₂ and GR will greatly retard the recombination of photoinduced charge carriers and prolong electron lifetime, which contribute to the enhancement of photocatalytic performance. The results of this research highlighted the fabrication of the TiO₂-GR nanocomposite as an efficient multifunctional photocatalyst for the degradation of hazardous compounds in waste water.

Acknowledgements

Financial support from the University Grants Commission (UGC), Government of India in the form of Major Research Project (MRP) is gratefully acknowledged by the authors.

Reference

- Qu, X.; Alvarez, P.J.J.; Li, Q. *Water Res.* **2013**, *47*, 3931-3946. DOI: [10.1016/j.watres.2012.09.058](https://doi.org/10.1016/j.watres.2012.09.058)
- Ibrahim Gaya, U.; Halim Abdullah, A. *J. Photochem. Photobiol. C: Photochem. Rev.* **2008**, *9*, 1-12. DOI: [10.1016/j.jphotochemrev.2007.12.003](https://doi.org/10.1016/j.jphotochemrev.2007.12.003)
- Tiwari, A.; Mishra, A.K.; Kobayashi, H.; Turner, A.P.F. (Eds), In *Intelligent Nanomaterials*, WILEY-Scrivener Publishing LLC, USA, **2012**.
- Maeda, K. *J. Photochem. Photobiol. C: Photochem. Rev.* **2011**, *12*, 237-268. DOI: [10.1016/j.jphotochemrev.2011.07.001](https://doi.org/10.1016/j.jphotochemrev.2011.07.001)
- Mathew, A.; Gowravaram, M.R.; Nookala, M. *Adv. Mater. Lett.* **2013**, *4*, 737-741. DOI: [10.5185/amlett.2013.2423](https://doi.org/10.5185/amlett.2013.2423)
- Ochiai, T.; Fujishima, A. *J. Photochem. Photobiol. C: Photochem. Rev.* **2012**, *13*, 247-262.

- DOI: [org/10.1016/j.jphotochemrev.2012.07.001](https://doi.org/10.1016/j.jphotochemrev.2012.07.001)
Imani, R.; Igljč, A.; Turner, A.P.F.; Tiwari, A. *Electrochemistry Communications*, **2014**, 40, 84-87.
5. Park, H.; Park, Y.; Kim, W.; Choi, W. *J. Photochem. Photobiol. C: Photochem. Rev.* **2013**, 15, 1–20.
DOI: [org/10.1016/j.jphotochemrev.2012.10.001](https://doi.org/10.1016/j.jphotochemrev.2012.10.001)
6. Zhang, B.T.; Zheng, X.; Li, H-F.; Lin, J-M. *Anal. Chim. Acta* **2013**, 784, 1–17.
DOI: doi.org/10.1016/j.aca.2013.03.054
Tiwari, A.; Shukla, S.K. (Ed.), In *Advanced Carbon Materials and Technology*, WILEY-Scrivener Publishing LLC, USA, **2014**.
7. An, X.; Yu, J.C. *RSC Adv.* **2011**, 1, 1426–1434.
DOI: [10.1039/C1RA00382H](https://doi.org/10.1039/C1RA00382H)
Parlak, O.; Turner, A.P.F.; Tiwari, A. *Advanced Materials*, **2014**, 26, 482-486.
Chaturvedi, A.; Tiwari, A.; Tiwari, A. *Advanced Materials Letters*, **2013**, 4, 656-661.
Parlak, O.; Tiwari, A.; Turner, A.P.F.; Tiwari, A. *Biosensors and Bioelectronics*, **2013**, 49, 53-62.
Tyagi, J.; Kakkar, R. *Advanced Materials Letters*, **2013**, 4, 721-736.
DOI: [10.5185/amlett.2013.3438](https://doi.org/10.5185/amlett.2013.3438)
8. Bai, S.; Shen, X. *RSC Adv.* **2012**, 2, 64–98.
DOI: [10.1039/C1RA00260K](https://doi.org/10.1039/C1RA00260K)
9. Xiang, Q.; Yu, J.; Jaroniec, M. *Chem. Soc. Rev.* **2012**, 41, 782–796.
DOI: [10.1039/C1CS15172J](https://doi.org/10.1039/C1CS15172J)
10. Huang, X.; Qi, X.; Boey, F.; Zhang, H. *Chem. Soc. Rev.* **2012**, 41, 666–686.
DOI: [10.1039/C1CS15078B](https://doi.org/10.1039/C1CS15078B)
11. Tiwari, A. *Adv. Mat. Lett.* **2012**, 3, 172-173
DOI: [10.5185/amlett.2012.2002](https://doi.org/10.5185/amlett.2012.2002)
12. Tyagi, J.; Kakkar, R. *Adv. Mat. Lett.* **2013**, 4(10), 721-736.
DOI: [10.5185/amlett.2013.3438](https://doi.org/10.5185/amlett.2013.3438)
13. Muthirulan, P.; Nirmala Devi, C.; Sundaram, M. *Arab. J. Chem.* **2013**, Article in press.
DOI: [org/10.1016/j.arabj.2013.04.028](https://doi.org/10.1016/j.arabj.2013.04.028)
14. Muthirulan, P.; Sundaram, M.; Kannan, N. *J. Adv. Res.* **2012**, 4(6), 479-484.
DOI: [org/10.1016/j.jare.2012.08.005](https://doi.org/10.1016/j.jare.2012.08.005)
15. Bai, X.; Wang, L.; Zhu, Y. *ACS Catal.* **2012**, 2, 2769–2778.
DOI: [org/10.1021/cs3005852](https://doi.org/10.1021/cs3005852)
16. Min, Y.L.; Zhang, K.; Zhao, W.; Zheng, F.C.; Chen, Y.C.; Zhang, Y.G. *Chem. Eng. J.* **2012**, 193–194, 203–210.
DOI: [org/10.1016/j.cej.2012.04.047](https://doi.org/10.1016/j.cej.2012.04.047)
17. Arif Sher Shah, M.S.; Park, R.; Zhang, K.; Park, J.H.; Yoo, P.J. *ACS Appl. Mater. Interfaces*, **2012**, 4, 3893–3901.
DOI: [org/10.1021/am301287m](https://doi.org/10.1021/am301287m)
18. Anandan, S.; NarasingaRao, T.; Sathish, M.; Rangappa, D.; Honma, I.; Miyauchi, M. *ACS Appl. Mater. Interfaces*, **2013**, 5, 207–212.
DOI: [org/10.1021/am302557z](https://doi.org/10.1021/am302557z)
19. Ye, A.; Fan, W.; Zhang, Q.; Deng, W.; Wang, Y. *Catal. Sci. Technol.* **2012**, 2, 969–978.
DOI: [10.1039/c2cy20027a](https://doi.org/10.1039/c2cy20027a)
20. Zhao, D.; Sheng, G.; Chen, C.; Wang, X. *App. Catal. B: Environ.* **2012**, 111–112, 303–308.
DOI: [org/10.1016/j.apcatb.2011.10.012](https://doi.org/10.1016/j.apcatb.2011.10.012)
21. Pastrana-Martínez, L.M.; Morales-Torres, S.; Likodimos, V.; Figueiredo, J.L.; Faria, J.L.; Falaras, P.; Silva, A.M.T. *App. Catal. B: Environ.* **2012**, 123–124, 241–256.
DOI: [org/10.1016/j.apcatb.2012.04.045](https://doi.org/10.1016/j.apcatb.2012.04.045)
22. Jiang, B.; Tian, C.; Pan, Q.; Jiang, Z.; Wang, J-Q.; Yan, W.; Fu, H. *J. Phys. Chem. C*, **2011**, 115, 23718–23725.
DOI: [org/10.1021/jp207624x](https://doi.org/10.1021/jp207624x)
23. Wang, F.; Zhang, K. *J. Mol. Catal. A: Chem.* **2011**, 345, 101–107.
DOI: [org/10.1016/j.molcata.2011.05.026](https://doi.org/10.1016/j.molcata.2011.05.026)
24. Zhang, H.; Zong, R.; Zhao, J.; Zhu, Y. *Environ. Sci. Technol.* **2008**, 42, 3803–3807.
DOI: [10.1021/es703037x](https://doi.org/10.1021/es703037x)
25. Zhang, H.; Zong, R.; Zhao, J.; Zhu, Y. *J. Phys. Chem. C* **2009**, 113, 4605–4611
DOI: [10.1021/jp810748u](https://doi.org/10.1021/jp810748u)
26. Ghorai, T.K.; Dhak, P. *Adv. Mat. Lett.* **2013**, 4, 121-130.
DOI: [10.5185/amlett.2012.7382](https://doi.org/10.5185/amlett.2012.7382)
27. Duhan, S.; Dehiya, B. S.; Tomer, V. *Adv. Mat. Lett.* **2013**, 4, 317-322.
DOI: [10.5185/amlett.2012.8414](https://doi.org/10.5185/amlett.2012.8414)
28. Zuas, O.; Budiman, H.; Hamim, N. *Adv. Mat. Lett.* **2013**, 4(9), 662-667.
DOI: [10.5185/amlett.2012.12490](https://doi.org/10.5185/amlett.2012.12490)

Advanced Materials Letters

Publish your article in this journal

ADVANCED MATERIALS Letters is an international journal published quarterly. The journal is intended to provide top-quality peer-reviewed research papers in the fascinating field of materials science particularly in the area of structure, synthesis and processing, characterization, advanced-state properties, and applications of materials. All articles are indexed on various databases including [DOAJ](https://www.doaj.org) and are available for download for free. The manuscript management system is completely electronic and has fast and fair peer-review process. The journal includes review articles, research articles, notes, letter to editor and short communications.

